Crystal Growth

Control of Biomineralization Dynamics by Interfacial Energies**

*Ruikang Tang, Molly Darragh, Christine A. Orme, Xiangying Guan, John R. Hoyer, and George H. Nancollas**

The constructive interaction of an inorganic crystal phase with an organic matrix results in the formation of composite biomaterials that have an exceptional appearance and remarkable physical properties.[1–4] During this process, living organisms may make use of peptides and proteins to deterministically modify nucleation, growth kinetics, surface morphology, and facet stability.[5–7] This control can range from the most specific binding of protein or macromolecular functional groups, to a nonspecific control, in which the species in solution change the thermodynamic driving force of crystallization.[6–8] It is generally agreed that proteins which are most active in the mediation of biologically directed mineral growth contain acidic amino acid residues, specifically, regions rich in carboxylates that interact with mineral surfaces to influence both the crystal morphologies and rates of formation.[7,9–11]

The mechanisms of biomineralization have been the subject of extensive discussion. A widely accepted view is that the organic matrix or the other molecules control the crystal structure by epitaxial matching.[6,8] Another suggestion is that the adsorption of additives does not occur on crystal faces but rather on dislocation lines for crystal growth or dissolution, which influences their morphology and rates of movement.[11,12] In this step-control model, the altered crystal shape is the result of dynamic processes, and the resulting crystal geometries are based on these modified surface steps. Herein, we report on a new mechanism based on modifications that result from a change of solid–solution interfacial energies. In this third mechanism, the adsorption of structure-controlling molecules may not influence the step dynamics.

A constant composition (CC) method sensitive to changes at the nanomolar level provides reliable rates of crystal growth,[13] and the development of in situ fluid atomic force microscopy (AFM) enables the visualization of these processes in real time. Brushite (dicalcium phosphate dihydrate, $CaHPO_4{\cdot}2H_2O$) is one of the more important mineral phases that has frequently been invoked as a precursor phase in the biological formation of apatite.[14] It is readily crystallized from aqueous solutions and has been found in developing bone, immature dentins, and even in renal stones.[15] It is also a good model system for biominerals as it is very stable with respect to structural rearrangements and the crystals are large enough to be employed as substrates for dynamic AFM examination. Citric acid, $HOOC(CH_2)_2CH(COOH)(CH_2)_2COOH$, a carboxylate-rich molecule, is often considered as a model system for more complicated naturally occurring proteins.[11] Deficiencies of urinary citrate predispose one to renal stone formation.[16] We expect that the general trends found for this model brushite–citrate system will also hold for the other crystallizing biominerals.

Figure 1 shows typical CC curves for brushite growth in the absence and presence of citrate. The normalized brushite-growth rate R in the absence of an additive is almost unchanged at citrate concentrations below 1.0×10^{-6} M ($R = 4.20\pm0.15\times10^{-5}\,\mathrm{mol\,m^{-2}\,min^{-1}}$). However, the rate is reduced by about 50% ($R = 2.08\pm0.05\times10^{-5}\,\mathrm{mol\,m^{-2}\,min^{-1}}$) in the presence of 2.1×10^{-6} M citrate, and the degree of inhibition increases with increasing citrate concentration to $0.22\pm0.01\times10^{-5}\,\mathrm{mol\,m^{-2}\,min^{-1}}$ or 95% inhibition at a citrate concentration of 1.0×10^{-5} M. A further increase in citrate concentration does not change the CC growth curves, which suggests that the maximum degree of inhibition by citrate is about 95%. It is important to note that as the ratios of calcium

[*] R. Tang, X. Guan, Prof. G. H. Nancollas
Department of Chemistry, University at Buffalo
The State University of New York
Buffalo, NY 14260 (USA)
Fax: (+1) 716-645-6947
E-mail: ghn@buffalo.edu
R. Tang
Department of Chemistry, Zhejiang University
Hangzhou, Zhejiang 310027 (China)
M. Darragh, C. A. Orme
Department of Chemistry and Materials Science
Lawrence Livermore National Laboratory
Livermore, CA 94551 (USA)
J. R. Hoyer
The Children's Hospital of Philadelphia
University of Pennsylvania, School of Medicine
Philadelphia, PA 19104 (USA)

[**] This work was supported by the National Institutes of Health (NIDCR grant number DE03223).

  DOI: 10.1002/ange.200500153

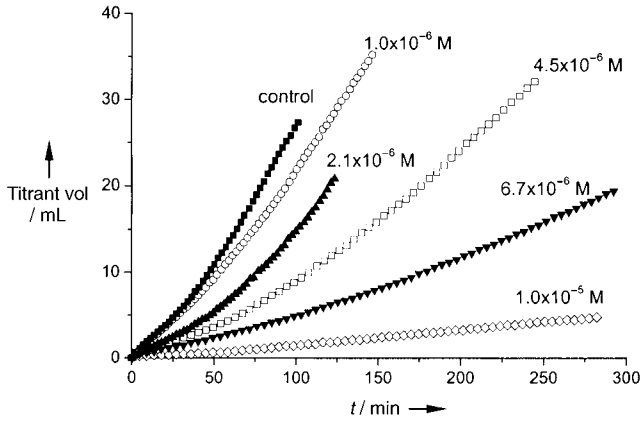

Figure 1. CC growth curves of brushite in the presence of citrate. The relative supersaturation with respect to brushite (σ) was 0.250; the pH value and ionic strength were 5.60 and 0.15 M, respectively; the curves have been normalized to the same seed mass of 10.0 mg. The growth rates are calculated from the gradient of these CC curves.

to citrate in the reaction solutions are always greater than 800, changes in the calcium concentration as a result of the formation of calcium citrate complexes can be ruled out. Thus, citrate effectively retards the growth of brushite crystals.

Typical platelike brushite crystals with smooth (010) surfaces served as suitable substrates for AFM (the Miller indices (*hkl*) denote a single plane and [*uvw*] specify a unique vector direction). In common with observations of other solution-based crystals growing near equilibrium,[11,12,17–19] parallel in situ AFM experiments, made under the same conditions as those for the CC experiments, show that brushite crystals in pure solutions grow on atomic steps generated at complex dislocation hillocks (Figure 2). These are triangular in shape with crystallographically distinct steps along the [101], [201], and [001] directions (Figure 2). In pure supersaturated solution, they have anisotropic spreading velocities in the order $[101] \approx [001] > [201]$, which is also reflected by the different terrace spacings between the growing steps.[11]

Qiu et al. and Orme et al. have proposed that the modification of biological mineralization (step control) is a result of additive binding at step edges to change the step velocities and morphologies.[11,12] However, in the present study of brushite biomineralization, neither the step morphology (Figure 2) nor the kinetics are affected by the presence of citrate even though it has been recognized as an effective inhibitor. At each of the citrate concentrations examined, neither defect nor the loss of defined direction for any of the three steps is observed in the AFM investigations performed in situ. Furthermore, the velocities of all three steps are not significantly changed in the presence of citrate (Figure 3). It is interesting that such a decrease in the crystal growth rate and change of crystal habit would be attributed conventionally to a decrease in step-spreading speed,[11,12] thus emphasizing that the pinned defects on the steps are consequences of the specific binding/adsorption of additives with resulting growth modification. Although the measured step velocities are not perfectly constant, the maximum variation is only about 10%. Nevertheless, in the parallel CC experiments, the bulk inhibition reaches more than 50%, so the conventional understanding of growth inhibition in terms of reduced step velocity does not apply.

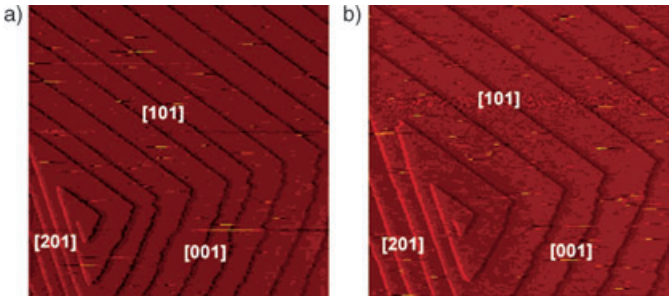

Figure 2. AFM frames of a growing (010)-brushite face: a) in the absence of citrate; b) in the presence of citrate. Introduction of citrate molecules reduces the brushite growth rate by changing the terrace spacing between the growth steps rather than the morphology or velocity of the steps, which results in a marked decrease of the step density on the growing surface.

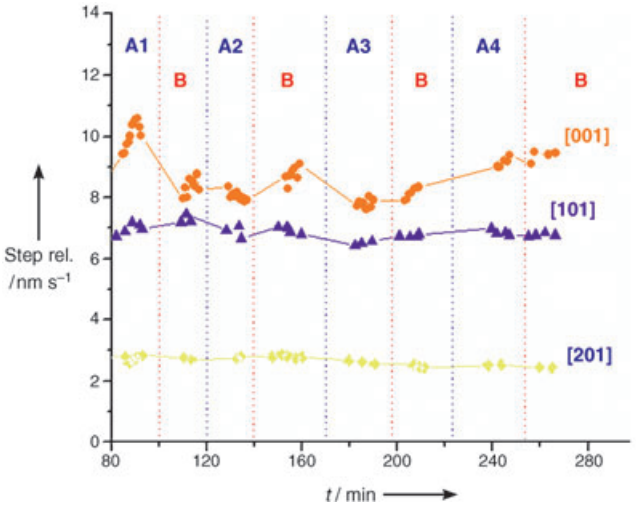

Figure 3. Evolution of the velocities of all three steps for crystals grown in solutions with and without citrate. All experimental conditions were kept constant, and there was no change in the spreading rates of steps in the absence and presence of citrate. The vertical red dotted lines indicate the time at which the crystals were exposed to a pure growth solution supersaturated with calcium phosphate (marked as B areas), while the blue dotted lines indicate the times at which the growth solutions contained citrate. In areas A1, A2, A3, and A4, the citrate concentrations were 1.0×10^{-6}, 5.0×10^{-6}, 1.0×10^{-5}, and 2.0×10^{-5} M, respectively.

It is noteworthy that citrate dramatically decreases the step density, especially for the [101] and [001] steps (Figure 2). It is well-known that the bulk growth rate R depends not only upon the step velocity but also upon the step density.[17–19] R is dominated by the two fastest growth steps ([101] and [001] steps), and the decrease in step density accounts for the observed inhibition in the bulk CC seeded growth experiments. Thus, the retardant effect is attributed to a decrease of step velocity. However, these modifications in step density are

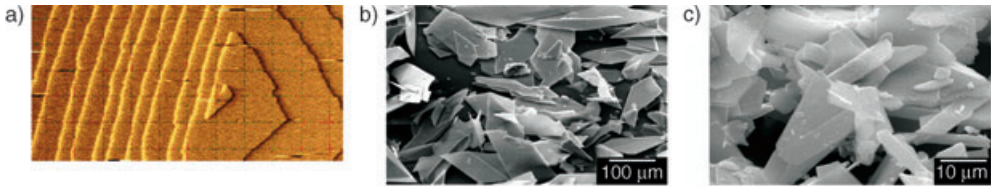

Figure 4. a) AFM image shows that inhibition effects (decreasing step density) are anisotropic; increasing citrate concentration (5.0×10^{-5} M) results in density reductions of fast growth steps [101] and [001], which are much more significant than that of the slow growth step [201]. In bulk crystallization experiments, the morphologies of grown brushite crystallites change from typical platelike (b) to rodlike (c) at high citrate concentrations (1.0×10^{-5} M) as a result of this anisotropic modification.

anisotropic; the ratio of [101] or [001] step spacings to those of [201] increases with increasing citrate (Figure 4a), which implies that the inhibition order is $[101]\approx[001]>[201]$. It follows that although [201] steps have the lowest growth rate in the control experiments, they are much less influenced by the presence of citrate than the [101] and [100] steps. With increasing citrate concentration and greater inhibition on [001] and [101] steps, the growth of [201] steps eventually dominates. At higher concentrations of citrate (1.0×10^{-5} M), the effective growth in the [001] and [101] directions decreases markedly and, as expected, the typical platelike brushite crystallites become rodlike (Figure 4b,c). The much lower inhibitory influence on the [201] steps also explains why citrate cannot fully inhibit brushite CC growth rates. Our results are in general agreement with the essential role of step modification in biomineralization. However, there is one important new feature: the results clearly show that biological systems may use step density rather than step velocity to change mineralization rates by modifying step energies while the velocity and morphology are virtually unchanged.

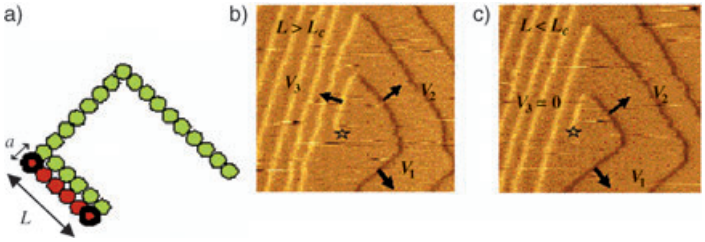

Figure 5. a) Enlargement of a dislocation source; the green represents the original step while the orange represents the new growth. The images in b) and c) show that the critical length is the minimum length at which the step will begin growing outward and the following step will begin growing. Adding biological additives such as citrate, and thus altering the energetics of the crystal formation, can in turn alter the shape of the crystal. The dislocation source on brushite surface is marked with a star.

Crystal growth in solution occurs at surface dislocations, which provide constant sources of steps.[17] Two terms that determine whether a step will grow or dissolve are related to the solution supersaturation S and the free energy of the step edge. The total change in free energy of the system is given by Equation (1). Here, n is the number of growth units adsorbing

$$\Delta G = -n\,\Delta\mu + 2a\gamma_{step} \qquad (1)$$

to the surface and $\Delta\mu$ is the change in chemical potential per growth unit during this phase transformation ($\Delta\mu \propto \ln S$). The second term relates the free energy of the step edge γ_{step} and the diameter a of the newly added growth units. The diagram (Figure 5a) shows the relationship between n and the step length such that $n = L/a$. The addition of molecules to a step becomes favorable at the point at which $\Delta G \leq 0$. Solving for L gives the critical length L_C, the length at which the step will begin growing outward and the following step will develop (Figure 5b,c). The spontaneous step growth does not occur until L_C is reached; rather, it will remain stationary or dissolve with no contribution to the growth rate. In this way, the mass of a brushite crystal increases as calcium and phosphate ions are deposited along steps on the crystal surfaces. These steps grow by spiraling outward from the dislocation sources on the surface. The relationship between terrace widths for the steps and the critical length L_C has been discussed.[18,19] Figure 2b suggests that citrate increases L_C, and in turn increases the period of time that it takes for a dislocation to create new step edges (this conclusion is supported by the nucleation study described below). As the step velocity is not inhibited by citrate, the terrace widths become larger and the step density is decreased on the growing (010) brushite surfaces. In Equation (1), when the supersaturation is kept constant, the only variable that can influence the value of L_C is the step energy, γ_{step}. It follows that γ_{step} is modified by the presence of citrate in the solution.

To further test this model, we have measured the interfacial tensions of brushite surfaces in the solutions by using a thin-layer wicking (TLW) method.[20] As predicted, the results, which are summarized in Table 1, show that the adsorption of citrate increases the interfacial energy γ_{SL} of brushite. In terms of an isotropic model γ_{step}, the mean value for all crystal-plane-step energies can be considered to be a

Table 1: Influence of citrate on brushite interfacial tension γ_{SL}. The increasing surface tension values and induction times (τ) in supersaturated brushite solutions with increasing citrate concentration are in agreement with Equation (3).

	γ_{SL} [mJ m^{-2}]	$\tau_\sigma = 0.450$ [min]
Control	4.53	≈400
2.0×10^{-6} M citrate	5.96	≈560
5.0×10^{-6} M citrate	7.06	≈760
1.0×10^{-5} M citrate	8.87	≈1100

function of γ_{SL}. In an analogous relationship between γ_{step} and L_C for steps at the microscopic level, the Kelvin–Gibbs equation [Eq. (2)] expresses the dependence, on a macro-

$$r^* = \frac{2\gamma_{SL}\,\Omega}{kT\ln S} \tag{2}$$

scopic scale, of the energy of formation of nucleated droplets of minimum radius r^* (assuming spherical shape) and surface tension γ_{SL}. In Equation (2), Ω is the volume occupied by each growth unit. It implies that spontaneous crystallization does not occur in bulk until critical conditions are reached, or the driving force (supersaturation) is sufficiently high. Rather, a metastable equilibrium condition persists during an "induction period" τ prior to crystal formation. If the simplifying assumption is made that τ is essentially concerned with classical nucleation, we can use Equation (3), in which, C_1 and

$$\ln\tau \propto \left[C_1 + C_2\frac{\gamma_{SL}^3}{k^3\,T^3\,(\ln S)^2}\right] \tag{3}$$

C_2 are independent constants. Equation (3) shows that the increase of the interfacial tension γ_{SL} following the introduction of citrate results in the inhibition of brushite growth and increase of the induction time.

Mann et al. suggested that the interaction of carboxyl groups with Ca^{2+} ions may increase the local concentration of a carboxylated additive in the vicinity of these cations, thereby lowering the energy barrier for nucleation and inducing the precipitation of calcium salts, such as calcium oxalate and calcite, in the "modified" supersaturated solutions.[1,6,8] In contrast, the CC nucleation results in the present study show that citrate dramatically increases the induction times and nucleation is retarded (Figure 6). The data in Table 1 further confirm the relationship between the induction time and surface tension as a function of citrate concentration. The data support the suggestion that citrate

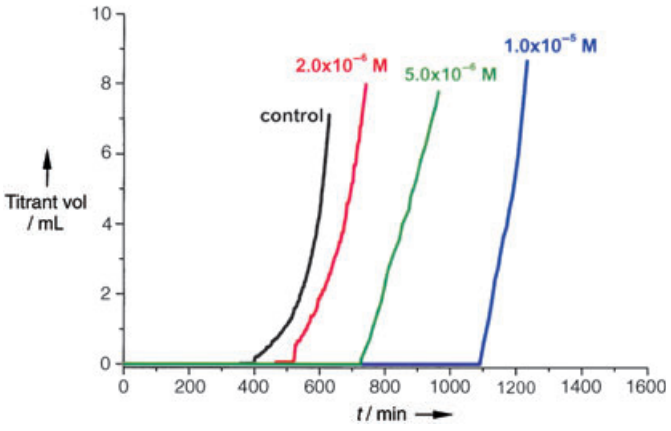

Figure 6. CC nucleation studies of brushite at different citrate concentrations. Although the carboxylate-rich molecules may bind to calcium ions in the solution to result in higher local concentrations near these molecules, the nucleation of brushite is not promoted by the mechanism of epitaxial control as suggested by Mann et al.[6,8] Instead, the longer nucleation induction times in the presence of citrate indicate that this carboxylate-rich compound is a nucleation inhibitor.

delays the formation of active step sources and increases the time for the formation of critical one-dimensional steps. In this process, interfacial energetic control plays the most important role as it can modify the critical conditions directly, as described by Equations (2) and (3). It is also well known that solution properties, such as surface tension, can be changed by the adsorption of additives. Although additives such as simple inorganic ions are unable to bind to the precipitated solid surfaces by an "epitaxial fit" or incorporate into the crystal lattice, the crystallization and morphology of the resulting crystals can be altered by these foreign additives. However, the interfacial energetic control can provide an interesting explanation of these modified crystallizations.

Our results suggest that the addition of biological growth modifiers alters mineral surface energies, thus changing the critical step length and delaying the formation of active steps for crystal growth. In bulk crystallization, these effects are manifested by longer induction times and delayed nucleation. We also conclude that the alteration of crystal habit may be because of the anisotropic modification of step densities in different growth directions and consequently changes of crystal geometry. These conclusions emphasize the importance of interfacial energies in biomineralization and their effect on critical step length. Approaches involving surface–step adsorption, for example by using a Langmuir model, may be misleading. This finding will be important for improving our understanding of the mechanisms of biomineralization.

Experimental Section

Constant composition for bulk-crystallization studies: This method can mimic in vivo biologically stabilized conditions for crystallization. Titrant solutions are added to maintain constant concentrations of the reaction solution during the experiments, and the kinetic growth results can be calculated from the addition rates of the titrant. Crystallization experiments were performed in double-walled Pyrex vessels with magnetic stirring (450 rpm). The supersaturated reaction solutions (200 mL) were prepared by mixing calcium chloride and potassium dihydrogen phosphate with sodium chloride to maintain the physiological ionic strength, $I = 0.15\ \mathrm{mol\,L^{-1}}$. The pH value was adjusted to 5.60 ± 0.01 with 0.1 M KOH solution. For experiments in the presence of additive, citrate solutions (1.00×10^{-4} or 1.00×10^{-3} M) were added prior to pH adjustment. Nitrogen presaturated with water vapor at 37 °C was passed through the reaction solutions to exclude carbon dioxide. The growth reactions were initiated by the introduction of brushite seed crystallites (10.0 mg); no seed was used for the CC nucleation experiments. Titrant addition was potentiometrically controlled using glass (Orion 91–01) and Ag/AgCl reference electrodes (Orion 900100). During crystallization, the electrode potential was constantly compared with a preset value, and the difference, or error signal, activated two motor-driven titrant burettes to maintain a constant thermodynamic driving force. Concentrations of the titrant solutions which were used to compensate reaction solutions for growth are given by Equations (4a) and (4b) for titrant burette no. 1 and Equations (5a) and (5b) for titrant burette no. 2. Here, W and T

$$T_{CaCl_2} = 2\,W_{CaCl_2} + C_{eff} \tag{4a}$$

$$T_{NaCl} = 2\,W_{NaCl} - 2\,C_{eff} \tag{4b}$$

$$T_{KH_2PO_4} = 2\,W_{KH_2PO_4} + C_{eff} \tag{5a}$$

$$T_{KOH} = 2\,W_{KOH} + 2\,W_{KOH} \tag{5b}$$

are the total concentrations in the reaction solutions and titrants, respectively, and C_{eff} is the effective titrant concentration with respect to brushite. During the reactions, slurry samples were periodically withdrawn and filtered, and the solutions were analyzed for calcium and phosphate. The total concentrations of calcium and phosphate remained constant to within $\pm 1.5\,\%$ during the experiments.

The growth flux rate R is calculated by using Equation (6), in

$$R = \frac{C_{eff}}{A_T}\frac{dV}{dt} \tag{6}$$

which C_{eff}, the effective titrant concentration with respect to brushite, indicates the molar amount of growth per liter of added titrants, dV/dt is the gradient of the CC titrant curves, and A_T is the surface area. The initial value of A_T was calculated from the specific surface area of the seed crystals, which was determined by Brunauer–Emmett–Teller (BET) nitrogen adsorption, and subsequent values were estimated from the growth model for brushite. Growth rates were calculated from the first 20 minutes of the reaction.

For the nucleation tests, the induction time τ was determined directly from the beginning of a steady and continuous addition of titrant solutions by CC.

Solution speciation and supersaturation: The supersaturation S and relative supersaturation σ are given by Equation (7), in which IP

$$\sigma = S - 1 = \left[\frac{IP}{K_s}\right]^{1/2} - 1 \tag{7}$$

is the ionic activity product, and the solubility activity product of brushite K_s is 2.36×10^{-5}. Solution speciation calculations were made by using the extended Debye–Hückel equation proposed by Davies[21] from mass balance expressions for total calcium and total phosphate with appropriate equilibrium constants by successive approximation for the ionic strength.

In situ atomic force microscopy: AFM images were collected in contact mode with a Digital Instruments Nanoscope III instrument. All images were acquired in height and deflection modes by using the lowest tip force possible to reduce the tip–surface interaction. The brushite seed crystal was anchored inside the fluid cell, and supersaturated solutions (identical to the CC reaction solutions) were passed through it while the images were taken.

Scanning electron microscopy (SEM): Samples under vacuum were sputter-coated with a thin carbon deposit to provide conductivity and then examined with a field-emission SEM (Hitachi S-4000), typically at 20 or 30 KeV.

Received: January 14, 2005
Published online: May 6, 2005

Keywords: biomineralization · crystal growth · interfaces · materials science · surface chemistry

[1] S. Mann, D. D. Archibald, J. M. Didymus, T. Douglas, B. R. Heywood, F. C. Meldrum, N. J. Reeves, *Science* **1993**, *261*, 1286–1292.
[2] S. Weiner, H. D. Wagner, *Annu. Rev. Mater. Sci.* **1998**, *28*, 271–298.
[3] A. P. Alivisatos, *Science* **2000**, *289*, 736–737.
[4] A. Berman, J. Hanson, L. Leiserowitz, T. F. Koetzle, S. Weiner, L. Addadi, *Science* **1993**, *259*, 776–779.
[5] L. Addadi, L. J. Moradian, E. Shay, N. G. Maroudas, S. Weiner, *Proc. Natl. Acad. Sci. USA* **1987**, *84*, 2732–2736.
[6] S. Mann, J. M. Didymus, N. P. Sanderson, B. R. Heywood, E. J. A. Samper, *J. Chem. Soc. Faraday Trans.* **1990**, *86*, 1873–1880.
[7] A. Berman, L. Addadi, S. Weiner, *Nature* **1988**, *331*, 546–548.
[8] S. Mann, B. R. Heywood, S. Rajam, J. D. Birchall, *Nature* **1998**, *394*, 692.
[9] C. S. Sikes, M. L. Yeung, A. P. Wheeler, in *Surface Reactive Peptides and Polymers: Discovery and Commercialization*, ACS Symposium Series XIII (Eds.: C. S. Sikes, A. P.Wheeler), ACS Books, Washington DC, **1991**, p. 444.
[10] A. George, L. Bannon, B. Sabsay, J. W. Dillon, J. Malone, A. Veis, N. A. Jenkins, D. J. Gilbert, N. G. Copeland, *J. Biol. Chem.* **1996**, *271*, 32869–32871.
[11] S. R. Qiu, A. Wierzbicki, C. A. Orme, A. M. Cody, J. R. Hoyer, G. H. Nancollas, S. Zepeda, J. J. De Yoreo, *Proc. Natl. Acad. Sci. USA* **2004**, *101*, 1811–1815.
[12] C. A. Orme, A. Noy, A. Wierzbicki, M. T. McBride, M. Grantham, H. H. Teng, P. M. Dove, J. J. DeYoreo, *Nature* **2001**, *411*,775–779.
[13] M. B. Tomson, G. H. Nancollas, *Science* **1978**, *200*, 1059–1060.
[14] S. V. Dorozhkin, M. Epple, *Angew. Chem.* **2002**, *114*, 3260–3277; *Angew. Chem. Int. Ed.* **2002**, *41*, 3130–3146.
[15] R. Z. LeGeros, *Calcium Phosphates in Oral Biology and Medicine*, Karger, Basel, **1991**.
[16] C. Y. C. Pak, *Miner. Electrolyte Metab.* **1994**, *20*, 371–377.
[17] W. K. Burton, N. Cabrera, F. C. Frank, *Philos. Trans. R. Soc. London Ser. A* **1951**, *243*, 299–358.
[18] C. J. Cramer, D. G. Truhlar, *Science* **1992**, *256*, 213–217.
[19] H. H. Teng, P. M. Dove, C. A. Orme, J. J. De Yoreo, *Science* **1998**, *282*, 724–727.
[20] C. J. Van Oss, R. F. Giese, Z. Li, K. Murphy, J. Norris, M. K. Chaudhury, R. J. Good, *J. Adhes. Sci. Technol.* **1992**, *6*, 413–428. The values of γ_{SL}, determined by TLW methods, are always lower than those obtained by other surface-tension measurements as the double-layer effects are also included; see W. Wu, G. H. Nancollas, *Adv. Colloid Interface Sci.* **1999**, *79*, 229–279; however, all the determination methods reach the same conclusion that the brushite–solution interfacial energy is increased by citrate.
[21] C. W. Davies, *Ion Association*, Butterworth, London, **1962**.

